Journal of Alloys and Compounds 509 (2011) 1920–1923

Contents lists available at ScienceDirect

Journal of Alloys and Compounds

journal homepage: www.elsevier.com/locate/jallcom

Effects of milling methods on the dielectric and the mechanical properties of hot-pressed sintered $MoSi_2/Al_2O_3$ composites

Zhibin Huang[a,*], Wancheng Zhou[a], Xiufeng Tang[a], Jiankun Zhu[b]

[a] State Key Laboratory of Solidification Processing, School of Materials Science and Engineering, Northwestern Polytechnical University, Xi'an 710072, China
[b] JiangSu Province Ceramics Research Institute, YiXing 214221, China

ARTICLE INFO

Article history:
Received 6 July 2010
Received in revised form 11 October 2010
Accepted 21 October 2010
Available online 30 October 2010

Keywords:
Milling methods
$MoSi_2/Al_2O_3$ composites
Dielectric properties
Mechanical properties

ABSTRACT

Two different milling methods were used to fabricate $MoSi_2/Al_2O_3$ ceramic composites. The wet ball-milling technique was found to be more effective in dispersing $MoSi_2$ particles in Al_2O_3 matrix than the dry ball-milling technique. The dielectric and the mechanical properties were evaluated for the composites fabricated by the above two methods and the results were compared. Excellent mechanical properties were obtained from the composites fabricated by the wet ball-milling technique. However, it seems difficult to adjust the permittivity of the wet-milled composites where the $MoSi_2$ conductive networks are easier to form.

1. Introduction

In recent years, radar absorbing materials have attracted considerable attention both in commercial and military applications [1–4]. Electrical conductive fillers are usually incorporated into the insulating matrix to fabricate composites in radar absorbing applications [5–8].

$MoSi_2$ is one of the promising fillers which could be employed in electromagnetic wave-absorbing materials and paints because of its high electrical conductivity [9]. Many physical properties of $MoSi_2$ and its composites have been extensively studied in the past two decades [10–12]. However, it appears that there are few reports on the dielectric properties of $MoSi_2$ and its composites at GHz frequencies [13,14].

As to the insulating matrix, Al_2O_3 is an excellent choice for composites with $MoSi_2$ because Al_2O_3 in its α form is thermally compatible and has a very small coefficient of thermal expansion (CTE) mismatch with $MoSi_2$. Dense $MoSi_2/Al_2O_3$ composites have already been fabricated by sintering [15]. Furthermore, excellent mechanical properties such as high strength are also available in the $MoSi_2/Al_2O_3$ composites [16].

As we know, the filler dispersion has great influence on the performance of particle-filled composites [17]. Usually, the milling method resulting in a change in particle size distribution is considered to be a simple process for particle dispersion. However, in the presence of the particle-filled composites, effects of milling methods on the dielectric properties have not been reported yet. The aim of this paper is to investigate the effects of different milling methods on the dielectric properties of $MoSi_2/Al_2O_3$ composites. What is more, the mechanical properties are explored to evaluate the load-bearing capacity of the composites.

2. Experimental

2.1. Experimental materials

The starting materials were α-Al_2O_3 (Main phase content > 99.9 wt.%, D_{50} = 0.7 μm) produced by Zibo Dongchangye Alumina Ltd., China, and $MoSi_2$ produced by Liaoning Nitrogen Compound Co. Ltd., China. The average particle size of the $MoSi_2$ is about 1 μm, and 90% of the $MoSi_2$ particles are in the range of 1 ± 0.1 μm.

The α-Al_2O_3 and the $MoSi_2$ powders were proportionally weighted and then planetary ball-milled in two ways. One was wet ball-milling technique in ethanol (Series B) and the other was the dry ball-milling technique without any additives (Series A). The mixtures were then dried at 80 °C for 1 h and mechanically grinded in mortar for 1 h. The process flow chart following for fabricating the composites is shown in Fig. 1. Finally, the resulting mixtures were put into a graphite die and hot-press sintered in the vacuum furnace at 1600 °C for 1 h with the heating rate of 10 °C/min. The sintering temperature was 0.8 T_m (T_m: melting temperature) of the α-Al_2O_3, which was usually required for the sintering of a ceramic powders [18]. A 12.5 MPa load was applied to the graphite die before heating and when the temperature reached 1600 °C, the load was increased to 25 MPa and maintained at that level for 1 h. The sample codes and the component of starting materials are listed in Table 1.

2.2. Test methods

The densities of the sintered samples were measured by the Archimedes method. The Rockwell hardness of the sintered samples was measured using the 500RA (Wilson-Wolpert) hardness tester. The hardness tests were carried out

* Corresponding author. Tel.: +86 29 88494574; fax: +86 29 88494574.
E-mail address: huangzhibin83@163.com (Z. Huang).

0925-8388/$ – see front matter © 2010 Elsevier B.V. All rights reserved.
doi:10.1016/j.jallcom.2010.10.088

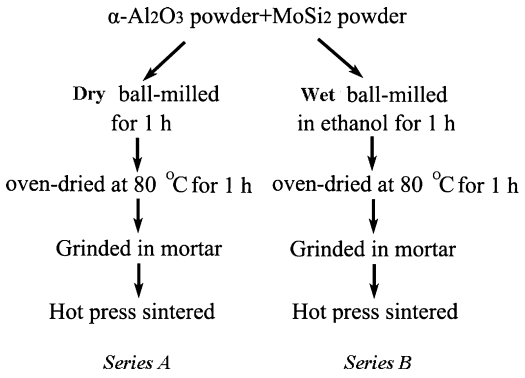

Fig. 1. Process flow chart followed for fabricating the composites.

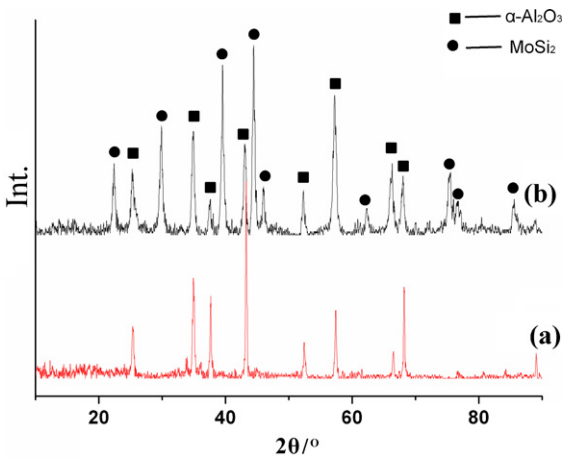

Fig. 2. XRD patterns of (a) Sample A0 (pure Al_2O_3) and (b) Sample B4 ($MoSi_2/Al_2O_3$ composite).

at 15 different positions of the sample surfaces, and the average values were calculated. The hot-pressed billets were cut into specimens with dimensions of 3 mm × 5 mm × 40 mm by a diamond grinding wheel for three-point bending strength test, in which the span is 30 mm and the crosshead speed is 0.5 mm/min. The measurements were carried out on the cross section of the samples, and the results were the average value from 4 samples. The fracture surfaces of the samples were observed by scanning electron microscopy. The complex dielectric constant between 8.2 and 12.4 GHz was measured by the waveguide method using E8362B PNA Series network analyzer, which requires specimens with dimensions of 10.16 mm × 22.86 mm × 2 mm. For a dielectric material ($\mu' = 1$, $\mu'' = 0$) the relative error varies between 1% (pure dielectric) and 10% (highly conductive materials). All the tests of the composites were evaluated at room temperature.

3. Results and discussion

3.1. Mechanical properties and microstructure

The densities of the samples are listed in Table 1. As can be seen, the relative density of pure Al_2O_3 sintered at 1600 °C achieves 99.18%, while it decreases dramatically when $MoSi_2$ is added, which means that the addition of $MoSi_2$ into Al_2O_3 is detrimental to the sintering when sintering additives are absent. The flexural strength data are also given in Table 1. It can be seen that all the composites exhibit a significantly higher strength than the unreinforced pure Al_2O_3. The flexural strengths of Samples A4 and B4 are about 22% and 66% higher than that of the pure Al_2O_3 respectively, which can be attributed to three factors. Firstly, the presence of the $MoSi_2$ particles results in the refinement of the grains of the Al_2O_3 matrix in the composites. Fig. 2 shows the XRD patterns of the pure Al_2O_3 and the $MoSi_2/Al_2O_3$ composites. It can be seen that the Al_2O_3 peaks of the pure Al_2O_3 ceramic are obviously narrower than those of the $MoSi_2/Al_2O_3$ composites, which proves that the grains size of the Al_2O_3 are refined after adding the $MoSi_2$ particles. The second factor is the load transfer from the matrix to the reinforcement phase. The load transfer is efficient in these composites because the interfaces are observed to be compact (as seen in Fig. 3f). In addition, the coefficients of thermal expansion (CTE) of $MoSi_2$ and Al_2O_3 differ by just 4% at elevated temperatures, hence the influences of the mismatch in CTE on the mechanical properties are small [9].

It is also important to note that the flexural strengths of the wet-milled composites (Series B) are higher than that of the dry-milled composites (Series A) due to the different dispersion situation of $MoSi_2$ particles in the matrix. It can be observed in Fig. 2 that the $MoSi_2$ particles in the composites of Series B disperse better than in Series A, especially in the composites with high $MoSi_2$ content. As we know, well-dispersed filler particles will be more efficient to refine the grains of the Al_2O_3 matrix, which is helpful to improve the flexural strength of the composites. Besides, the grain size and the amount of the agglomerations in series B are smaller than those in series A, which can be observed by comparing Fig. 3c with Fig. 3d. When load is applied to the composites, it is transferred through the particles. And the presence of these agglomerate phases in the matrix will cause non-uniform load transfer, resulting in the lower strength. Conversely, if the particles disperse homogeneously, high flexural strength is exhibited. On the other hand, high hardness is also obtained in the composites. This is not surprising because the hardness of the two starting materials is very high.

It can be concluded that high strength and high hardness are achieved in the $MoSi_2/Al_2O_3$ composites prepared by hot press sintering. The wet-milled method has a distinctive advantage over the dry-milled one in improving the flexural strength of the $MoSi_2/Al_2O_3$ composites.

3.2. Dielectric properties

Dielectric performances of the composites prepared by different milling methods are shown in Figs. 4 and 5. It can be observed that the permittivities of the composites are closely correlated with the

Table 1
The composition of starting materials and mechanical properties.

Sample codes	$MoSi_2$ content (vol.%)		Flexural strength (MPa)	Hardness (HRF)	Relative density (%)
	Dry milled	Wet milled			
A0	0	0	284(±11)	95.13(±0.92)	99.18
A1	13.7	0	311(±12)	93.79 (±3.51)	93.52
A2	21.4	0	352(±18)	93.03(±2.96)	93.55
A3	22.7	0	353(±15)	93.55(±2.37)	93.18
A4	29.8	0	347(±13)	91.78(±2.53)	92.57
B1	0	13.7	378(±10)	93.76(±1.41)	94.42
B2	0	21.4	436(±12)	93.54(±1.26)	94.14
B3	0	22.7	448(±13)	93.65(±3.21)	94.03
B4	0	29.8	471(±17)	92.55(±1.08)	94.16

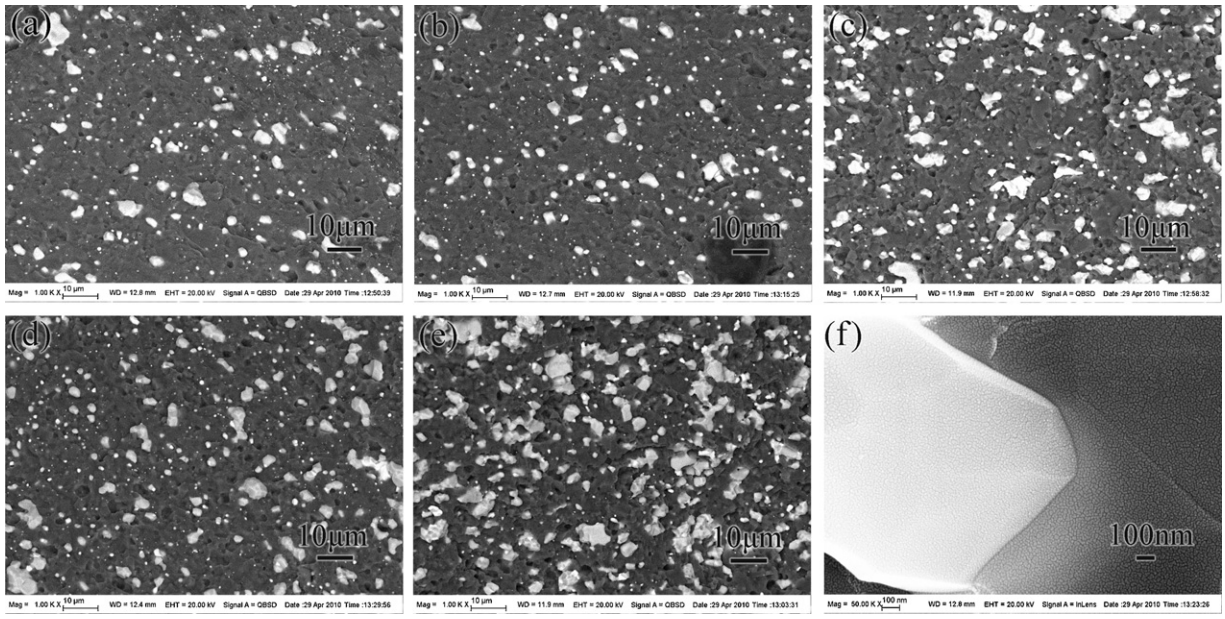

Fig. 3. SEM photographs of samples (a) Sample A1, (b) Sample B1, (c) Sample A3, (d) Sample B3, (e) Sample A4 and (f) an individual $MoSi_2$ particle surrounded by α-Al_2O_3 particle.

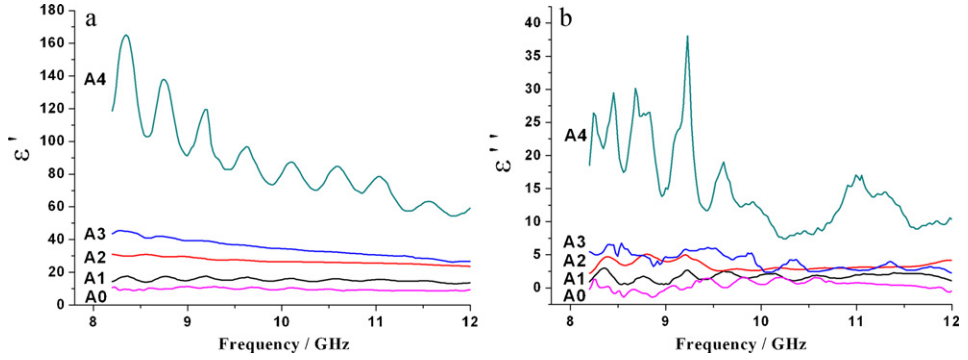

Fig. 4. (a) ε' and (b) ε'' of Series A vs. frequency.

volume fraction of $MoSi_2$. Both the real part (ε') and the imaginary part (ε'') of the complex permittivity rise over the whole frequency range with the increasing $MoSi_2$ content. Furthermore, by comparison with the composites containing lower $MoSi_2$ particles, it can be found that the fluctuation of the ε' and the ε'' of composites with high $MoSi_2$ particles are more visible. This fluctuation may be attributed to the high electric conductivity of the composites containing high $MoSi_2$ content.

A rapid increase in ε' can be seen both in Series A and Series B due to the gradually developing $MoSi_2$ conductive networks [19]. The average distance of the $MoSi_2$ particles has great influences on the formation of the conductive networks. When the interparticle distance is shorter than the gap width that quantum tunneling effect permits, conductive networks will form.

For blends with-dispersed spherical particles, Wut [20] assumed a simple cubic lattice to calculate the surface-to-surface interpar-

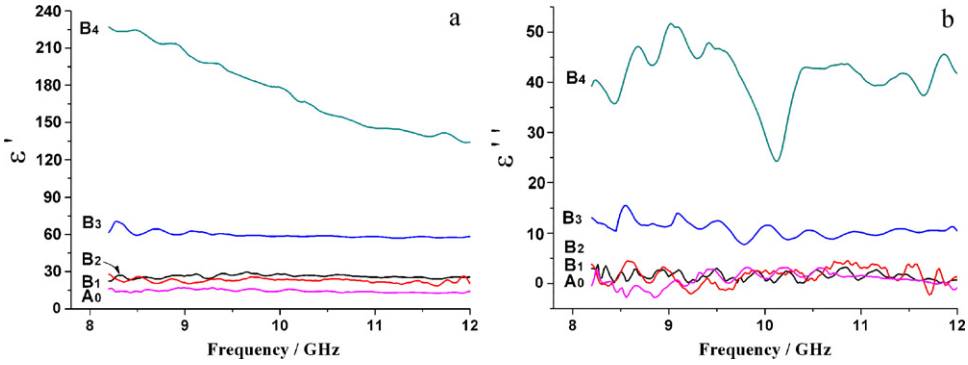

Fig. 5. (a) ε' and (b) ε'' of Series B vs. frequency.

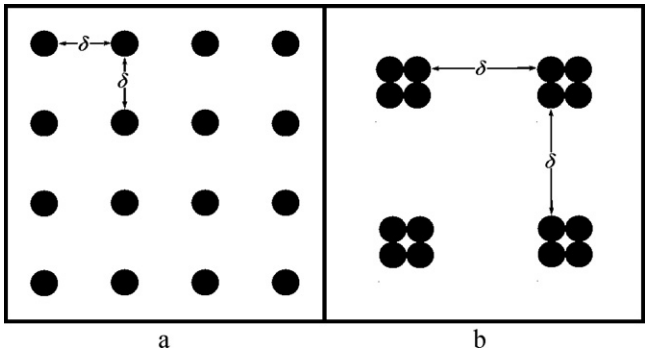

Fig. 6. The schematic of the (a) well dispersed and (b) worse dispersed $MoSi_2/Al_2O_3$ composites.

ticle distance by

$$\delta = D\left[\left(\frac{\pi}{6\varphi}\right)^{1/3} - 1\right] \quad (1)$$

where the δ is the average surface-to-surface interparticle distance, D is the particle diameter, φ is the volume fraction of particles. Eq. (1) shows that the δ of the $MoSi_2$ particles is dependent on the volume fraction as the particle diameter is constant. This can be observed in the SEM figures (Fig. 3) of the composites with different the $MoSi_2$ contents. The distances between the $MoSi_2$ particles are shortened by increasing the $MoSi_2$ content. At the same time, the $MoSi_2$ agglomerations also increase due to the increasing possibility of contact between $MoSi_2$ particles as the proportion of $MoSi_2$ increases.

It is also important to note that the rapid increase appears in Sample B3 when the $MoSi_2$ content reaches 22.7 vol.%, while it does not appear in Sample A3 with the same $MoSi_2$ content. In other words, more $MoSi_2$ is needed for dry-milled composites to form the conductive $MoSi_2$ networks (Sample A4). It suggests that the difference is ascribed to the influences of milling methods. As discussed above, the dispersion situation of the two types of samples is different, which is also a factor which the δ depends on. As shown in Fig. 6, the average surface-to-surface interparticle distance of filled particles in homogeneously dispersed composites is relatively short. It means that the well-dispersed $MoSi_2$ particles are more likely to reach the critical surface-to-surface interparticle distance (i.e. the electron hopping gap width) based on the Eq. (1). Obviously, the difference of dispersion situation arising from the milling methods plays an important role in the dielectric properties of the composites. The $MoSi_2$ particles in wet-milled composites are more prone to form conductive networks. Therefore, the rapid increase of ε' appears in the wet-milled composites when the $MoSi_2$ content reaches 22.7 vol.%, while it does not appear in dry-milled composites with the same $MoSi_2$ content.

On the other hand, the ε'' also increases with the increasing the $MoSi_2$ content in both Series A and Series B as shown in Figs. 4b and 5b. $MoSi_2$ is known as an intermetallic filler which has a metallic-type electrical conduction. It can be imaged that the average distance between the $MoSi_2$ particles will become shorter with the increasing $MoSi_2$ content, and the valence electrons can hop between more and more particles. As the $MoSi_2$ content exceeds the percolation limit, the composite will show a typical percolation behavior. Both the dielectric constant and the conductivity will increase drastically by several orders of magnitude, which is contributed by the valence electrons and those electrons located in the defect states [21–23]. Therefore, a rapid increase of ε'' appears in the composites when the conductive networks form in Samples A4 and B3.

Another mechanism which may contribute to the microwave energy loss is the contact resistance between $MoSi_2$ particles, which results in more energy conversion from microwave energy to thermal energy when the valence electrons with the same density pass through the joining points of the $MoSi_2$ particles.

4. Conclusions

In summary, the milling methods have great influences on the mechanical and dielectric properties of the $MoSi_2/Al_2O_3$ composites.

The wet ball-milling technical was found to be more effective to homogeneously disperse the $MoSi_2$ particles in the matrix, which is helpful to improve the flexural strength of the composites. While, the dielectric properties of the wet-milled composites seem difficult to adjust because the $MoSi_2$ conductive networks are easier to form in them. When the conductive network is formed, the valence electrons hop between more and more particles, resulting in the rapid increase of ε' and ε''.

The dielectric properties of the $MoSi_2/Al_2O_3$ composites can be adjusted by controlling the $MoSi_2$ content and the milling method. The dielectric and the mechanical properties can be tailored by choosing a suitable milling method. On the other hand, the flexural strength is also improved after the incorporation of $MoSi_2$ particles. $MoSi_2/Al_2O_3$ composite is a promising material in both the electromagnetic absorption characteristics and the load-bearing capacity aspects.

Acknowledgement

This work was financially supported by the fund of the States Key Laboratory of the Solidification Processing in NWPU, No. KP200901.

References

[1] I.M.De. Rosa, A. Dinescu, F. Sarasini, M.S. Sarto, A. Tamburrano, Compos. Sci. Technol. 70 (2010) 102.
[2] T. Zou, H. Li, N. Zhao, C. Shi, J. Alloys Compd. 496 (2010) L22.
[3] C. Wang, R. Lv, Z. Huang, F. Kang, J. Gu, J. Alloys Compd. (2010), doi:10.1016/j.jallcom.2010.09.078.
[4] Y Yang, C. Xu, Y. Xia, T. Wang, F. Li, J. Alloys Compd. 493 (2010) 549.
[5] Y.C. Qing, W.C. Zhou, F. Luo, D.M. Zhu, Phys. B – Condens. Matter 405 (2010) 1181.
[6] N.Q. Zhao, T.C. Zou, C.S. Shi, J.J. Li, W.K. Guo, Mater. Sci. Eng. B 127 (2006) 207.
[7] S. Ni, X. Wang, G. Zhou, F. Yang, J. Wang, D. He, J. Alloys Compd. 489 (2010) 252.
[8] H. Liu, H. Cheng, J. Wang, G. Tang, J. Alloys Compd. 491 (2010) 248.
[9] S. Kobel, J. Pluschke, U. Vogt, T.J. Graule, Ceram. Int. 30 (2004) 2105.
[10] K. Young, T. Ouchi, W. Mays, B. Reichman, M.A. Fetcenko, J. Alloys Compd. (2010), doi:10.1016/j.jallcom.20108.12.115.
[11] F. Baras, D.K. Kondepudi, F. Bernard, J. Alloys Compd. 505 (2010) 43.
[12] X. Fei, Y. Niu, H. Ji, L. Huang, X. Zheng, Ceram. Int. 36 (2010) 2235.
[13] M. Zakeri, R. Yazdani-Rad, M.H. Enayati, M.R. Rahimipoor, Mater. Sci. Eng. A – Struct. 430 (2006) 185.
[14] T. Watanabe, G.J. Zhang, X.M. Yue, Y.P. Zeng, K. Shobu, N. Bahlawane, Mater. Chem. Phys. 67 (2001) 256.
[15] A. Newman, S. Sampath, H. Herman, Mater. Sci. Eng. A – Struct. 261 (1999) 252.
[16] A. Chakraborty, S.V. Kamat, R. Mitra, K.K. Ray, J. Mater. Sci. 35 (2000) 3827.
[17] M. Hussain, Y. Oku, A. Nakahira, K. Niihara, Mater. Lett. 26 (1996) 177.
[18] P. Colomban, J. Mater. Res. 13 (1998) 803.
[19] P. Li, W.C. Zhou, J.K. Zhu, F. Luo, D.M. Zhu, Scripta Mater. 60 (2009) 760.
[20] A. Margolina, S. Wut, Polymer 29 (1988) 2170.
[21] S.C. Tjong, G.D. Liang, S.P. Bao, Scripta Mater. 57 (2007) 461.
[22] S. Ren, B. You, J. Du, X.J. Bai, J. Zhang, A. Hu, B. Zhang, X.X. Zhang, J. Alloys Compd. 465 (2008) 417.
[23] Z.-M. Dang, C.-W. Nan, D. Xie, Y.-H. Zhang, S.C. Tjong, Appl. Phys. Lett. 85 (2004) 97.